ISSN 0965-5425, Computational Mathematics and Mathematical Physics, 2010, Vol. 50, No. 4, pp. 711–720. © Pleiades Publishing, Ltd., 2010.
Original Russian Text © B.V. Arkhipov, V.N. Koterov, V.V. Solbakov, Yu.S. Yurezanskaya, 2010, published in Zhurnal Vychislitel'noi Matematiki i Matematicheskoi Fiziki, 2010, Vol. 50, No. 4, pp. 746–756.

Simulation of Suspended Substance Transport on the Continental Shelf: Computation of Soil Dumping in the Sea of Azov

B. V. Arkhipov, V. N. Koterov, V. V. Solbakov, and Yu. S. Yurezanskaya

Dorodnitsyn Computing Center, Russian Academy of Sciences, ul. Vavilova 40, Moscow, 119333 Russia

e-mail: arhip@ccas.ru, koterov@ccas.ru, july@ccas.ru

Received November 26, 2009

Abstract—Suspended substance dispersion in a water body is simulated in the case when the spread area is considerably larger than the depth of the water body. The performance and features of a previously proposed computational technique are demonstrated by computing the dispersion of mineral suspension clouds generated in the southern Sea of Azov in the course of soil dumping associated with repair work in the port of Temryuk. The results presented were obtained primarily in test computations aimed at the validation of the computational technique.

DOI: 10.1134/S0965542510040123

Key words: numerical methods, advection–diffusion equation, shelf, suspended substances, dumping, turbulent mixing, 4/3 power law, stochastic methods.

INTRODUCTION

The computation of the spread of mineral suspensions of complex fractional composition on shelves of marginal and inland seas is motivated by the need for assessments of anthropogenic impacts on the marine environment. The suspension concentration in sea water far away from a pollution source (far-field region) is low. Therefore, these substances can be viewed as a passive tracer whose fractions (i) spread independently of each other and (ii) do not dynamically influence the background water velocity field. These assumptions considerably simplify the problem. Nevertheless, there are a number of difficulties associated with the following points:

(i) The spread area of suspended substances is considerably larger than the depth of the water area.

(ii) The number of various suspension fractions is large, and their sedimentation velocities differ considerably from each other.

(iii) The concentrations at control points (1 mg/l), for which reliability has to be ensured by a numerical model, differ by five or more orders of magnitude from the suspension concentrations near the pollution source.

(iv) Vertical turbulent exchange and the adsorption properties of the bottom have a large effect on the sedimentation of fine suspended substances.

(v) The current velocity field can have a complex, spatially inhomogeneous, and reverse structure.

(vi) The horizontal turbulent exchange coefficient depends on the size of the diffusing object (the Richardson 4/3 law for the scattering of a compact suspension cloud in a turbulent medium (see [1, 2])).

(vii) Anthropogenic sources of suspended substances can persist for a long period (from several days to several months).

Intended for the simulation of suspended substance dispersion in a far-field region, an efficient computational technique taking into account the features listed above was proposed in [3, 4]. It is based on the following approaches:

(i) The three-dimensional advection–diffusion of polydisperse suspended substances generated by an instantaneous point source is reduced to a two-dimensional (depth-averaged) equation for a monodisperse suspension with a time-dependent effective deposition rate that takes into account vertical turbulent exchange and the adsorption properties of the bottom.

(ii) The superposition principle is used to simulate the effect of a continuous and/or distributed source of suspension.

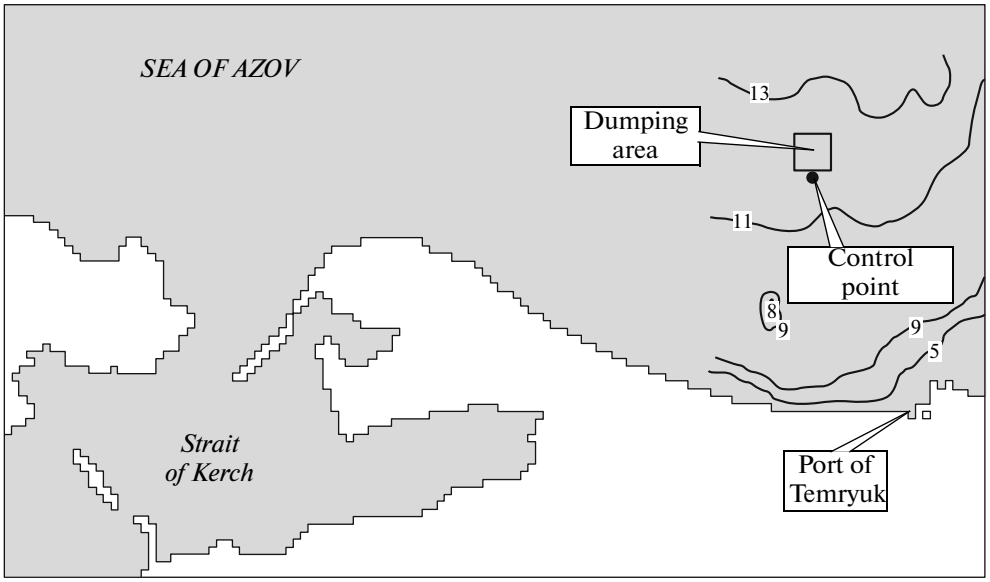

Fig. 1.

(iii) A stochastic discrete cloud method is developed that reproduces the Richardson 4/3 law in the computation of horizontal transport and dispersion of suspended substances.

This paper concludes [3, 4] and presents the results obtained by applying the developed technique to the simulation of the spread of suspended substances produced by soil dumping in the Sea of Azov in the course of dredging operations in the port of Temryuk. The initial data for the computations were somewhat simplified, but they generally reflected the dredging operations performed in the region, the hydrometeorological conditions, and the characteristics of bottom sedimentations.

The goal of this work is to demonstrate the performance of the substance dispersion technique as applied to a particular example and to validate the model by performing test computations.

1. THE OBJECT OF SIMULATION AND THE DAMPING SCENARIO

The port of Temryuk is located in the southern Gulf of Temryuk in the Sea of Azov (Fig. 1). Due to the natural conditions, the navigation ways in the region are silted up and have to be periodically recovered. Approximately half the amount of the soil excavated in dredging operations is dumped in the sea over a 3×3 km^2 dumping area (with a depth of $\approx$12 m) located to the northwest of the port (Fig. 1).

In the simulation of dumping, we assumed that soil is delivered to the dumping area by barges with a capacity of $M_0 = 265$ t. The dumping started in 4001 hours after the beginning of the year (corresponds to June 16) and terminated in 4202 hours (June 25). It was assumed that one barge is unloaded on the area every hour. The positions of 201 unloading points over the dumping area were specified using a random variable uniformly distributed in both coordinates. The soil taken to the dumping area was silt with a grain-size composition (see the table). Its mineral density was specified as $\rho_0 = 2650$ kg/m^3, and the porosity of the bottom sedimentations was assumed to be $\varepsilon_0 = 0.5$.

Each dumping event was simulated as an instantaneous distributed source of mineral suspension. The suspension concentration immediately after switching off this source was specified as

$$C_0 = \begin{cases} \dfrac{M_0}{2\pi(z_2 - z_1)\sigma'_{10}\sigma'_{20}} \exp\left(-\dfrac{x_1'^2}{2\sigma_{10}'^2} - \dfrac{x_2'^2}{2\sigma_{20}'^2}\right), & z_1 \le z \le z_2, \\ 0, \quad z < z_1, \quad z > z_2, \end{cases} \tag{1}$$

Table

Fractions	Range of particle diameters, mm	Mass fraction, %	Hydraulic coarseness, m/s
1	2.0–0.1	14.0	1.6E-1
2	0.1–0.05	36.0	4.5E-3
3	0.05–0.01	46.0	7.7E-4
4	0.01–0.005	2.8	4.9E-5
5	0.005–0.0001	1.2	5.6E-6

where the vertical coordinate z is measured from the free surface, $z_1 = 1$ m, $z_2 = 3$ m, the local coordinates x_1' and x_2' are measured from the dumping point in the direction of the water flow and in the perpendicular direction, $\sigma_{10}' = 5$ m, and $\sigma_{20}' = 2.5$ m (halves of the approximate sizes of the barge hold).[1]

2. HYDROLOGICAL CONDITIONS IN THE DAMPING REGION

To derive quantitative characteristics of the water currents in the region, we used the shallow water equations [5]

$$\frac{\partial h}{\partial t} + \frac{\partial hu_1}{\partial x_1} + \frac{\partial hu_2}{\partial x_2} = 0, \quad h = H + \eta,$$

$$\frac{\partial hu_1}{\partial t} + \frac{\partial hu_1^2}{\partial x_1} + \frac{\partial hu_1u_2}{\partial x_2} - fhu_2 = -\frac{\partial gh^2/2}{\partial x_1} + gh\frac{\partial H}{\partial x_1} + A\left(\frac{\partial^2 hu_1}{\partial x_1^2} + \frac{\partial^2 hu_1}{\partial x_2^2}\right) + \tau_1^0 + \tau_1,$$

$$\frac{\partial hu_2}{\partial t} + \frac{\partial hu_1u_2}{\partial x_1} + \frac{\partial hu_2^2}{\partial x_2} + fhu_1 = -\frac{\partial gh^2/2}{\partial x_2} + gh\frac{\partial H}{\partial x_2} + A\left(\frac{\partial^2 hu_2}{\partial x_1^2} + \frac{\partial^2 hu_2}{\partial x_2^2}\right) + \tau_2^0 + \tau_2.$$

Here, t is time; x_1 and x_2 are the Cartesian coordinates of a point $\mathbf{x}$ measured in the east and northern directions; u_1 and u_2 are the respective components of the current velocity $\mathbf{u}$; $f = 2\Omega\sin\varphi$ is the Coriolis parameter (where Ω is the angular velocity of the Earth and φ is the latitude of the place); H is the depth of the water area; η is the perturbation of the free surface level; g is the acceleration of gravity; A is the effective coefficient of horizontal turbulent momentum exchange; τ_1^0 and τ_2^0 are the wind stresses on the free surface, and τ_1 and τ_2 are the shear stresses at the bottom, which are usually specified by the quadratic friction law: $\tau_i = -\alpha|\mathbf{u}|u_i$, $i = 1, 2$ (α is the friction coefficient).

The water can be set into motion by specifying conditions on the open boundaries, where current and sea level data, including observational series, have to be used in the computations. Another driving force, which is especially important for current computations in inland seas, where the tidal phenomena are insignificant, is the wind stresses:

$$\tau_1^0 = |\boldsymbol{\tau}^0|\cos\theta, \quad \tau_2^0 = |\boldsymbol{\tau}^0|\sin\theta, \quad |\boldsymbol{\tau}^0| = (\rho_a/\rho_w)C_dV_{10}^2, \tag{2}$$

where ρ_a and ρ_w are the densities of air and water, respectively; V_{10} is the wind speed at 10 m above the free surface; θ is the angle between the x_1 axis and the wind direction, and the friction coefficient C_d is specified according to the following wind stress model (see [5]):

$$C_d = \begin{cases} 1.1 \times 10^{-3}, & V_{10} \le 6 \text{ m/s}, \\ (0.72 + 0.063V_{10}) \times 10^{-3}, & V_{10} > 6 \text{ m/s}. \end{cases}$$

[1] Instantaneous point sources of suspension were basically considered in [3, 4]. All the results are easily extended to the case of (1).

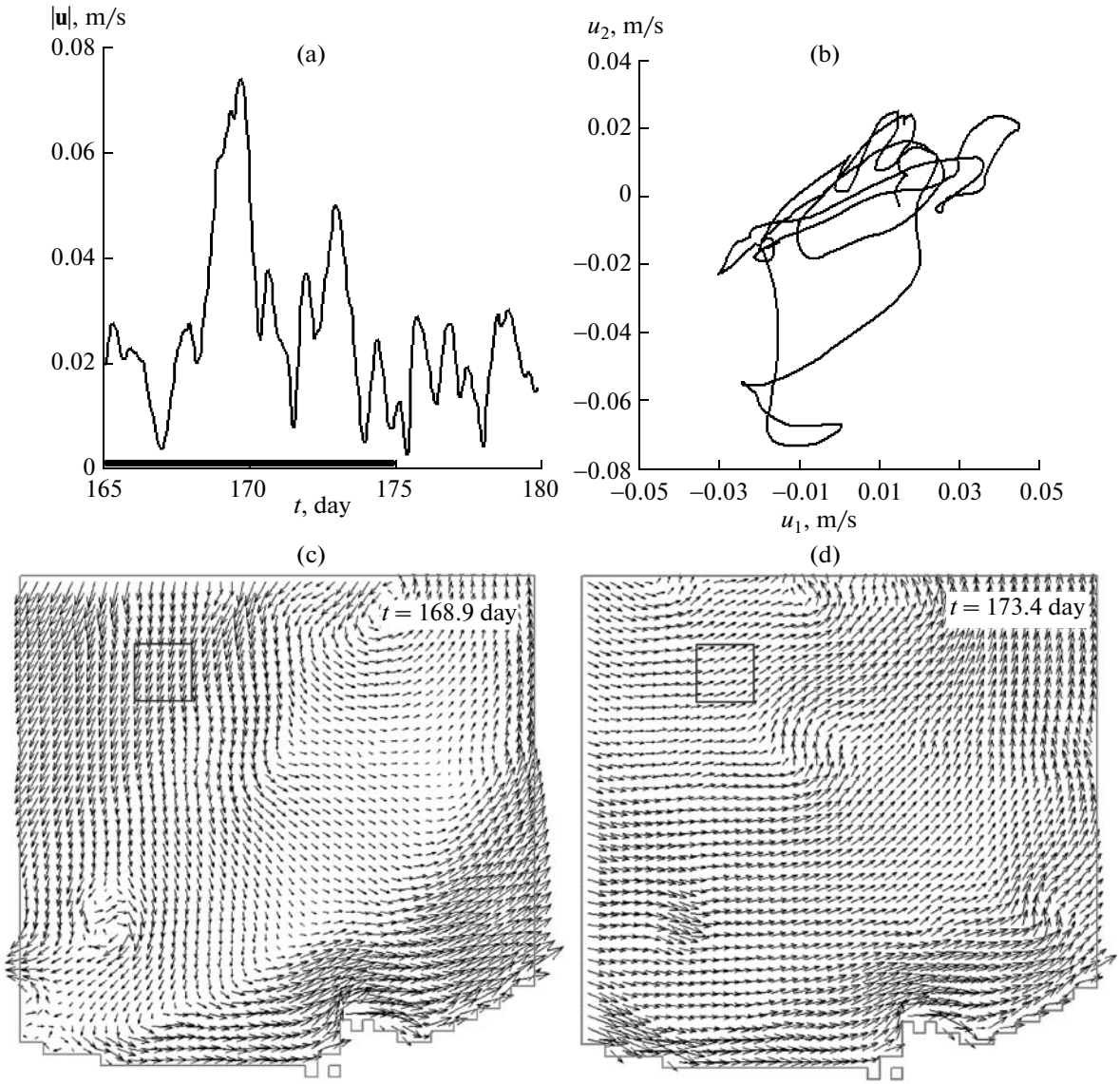

Fig. 2.

The current field was computed on a grid that completely covered the Sea of Azov with the Strait of Kerch and had an open boundary with the Black Sea (600×600 m^2 mesh cells, the domain consisted of 393×227 cells). Wind stresses (2) were computed using the 2.5-degree wind velocity data from the NCEP/NCAR reanalysis [6] for the 2005 summer.[2]

Figure 2 shows the numerical results. Specifically, Fig. 2a depicts the current speed at the center of the dumping area (the time interval during which soil was dumped is shown by the heavy line). The current velocity hodograph at the same point is presented in Fig. 2b. The instantaneous current velocity fields at two moments of time are shown in Figs. 2c and 2d. These computations were used in the simulation of suspended substance transport. The current velocity at an arbitrary point of the water area at an arbitrary time was derived by applying bilinear approximation in space and linear approximation in time.

Since no data were available on the typical horizontal turbulence structure in the region, in the computations (for the results, see below) we used the standard empirical model, according to which the horizontal turbulent dispersion of suspended substances in a cloud produced at the time t_0 by an instantaneous point source obeys the law $\sigma^2(t) = A_3(t - t_0)^3$, where $A_3 = 8 \times 10^{-9}$ m^2/s^3 (see [4]). In the computations, the

[2] http://www.esrl.noaa.gov/psd/data/gridded/data.ncep.reanalysis.html.

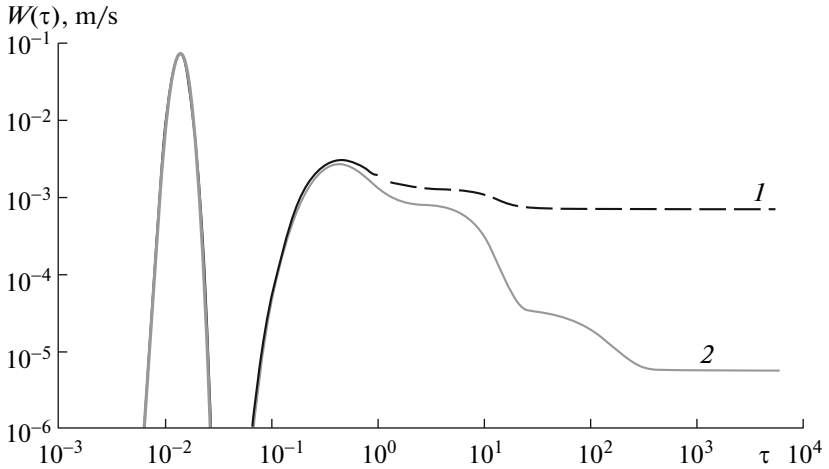

Fig. 3.

parameter γ in the longitudinal variance $K_D = \gamma H|\mathbf{u}|$ [4] ranged from 1 to 10 (according to [7], $\gamma = 0.45$ for the North Sea).

The characteristic rate of vertical turbulent diffusion was set equal to $u_* = 2.5 \times 10^{-3}$ m/s (the depth-averaged vertical turbulent exchange coefficient was $\overline{K}_z = 7.5 \times 10^{-3}$ m^2/s). The following two cases were considered:

(i) The bottom in neighborhood of the dumping area completely adsorbs the suspended substances.

(ii) There is no diffusive suspension flux at the bottom.

The first case can occur if the bottom is covered with sufficiently thick vegetation. The second case is a model of a bare bottom covered with a layer of friable fine-particle sediments.

3. EFFECTIVE HYDRAULIC COARSENESS OF SOIL

The calculated effective hydraulic coarseness [3] of the dumped soil is presented in Fig. 3. This characteristic determines the rate of variation in the total polydisperse suspension mass in a cloud produced by an instantaneous suspension source. The argument τ is the dimensionless time measured from the dumping moment t_0. It is defined by the expression

$$\tau = u_* \int_{t_0}^{t} H^{-1}(\mathbf{x}_0(t'))dt', \tag{3}$$

where $\mathbf{x}_0(t)$ is the trajectory of the cloud center.

The plots in Fig. 3 (see also the table) demonstrate the differential sedimentation character of various fractions in the suspension produced by soil dumping. At the first moments of time, the effective hydraulic coarseness is zero, since it takes some time even for the largest suspension particles to reach the bottom (the total suspension mass in the cloud does not vary over this time). Next, the suspension fractions are consecutively deposited, starting with the largest one (the first pronounced peak on the curve of $W(\tau)$ is explained by the features of the soil grain-size composition: the hydraulic coarsenesses of the first and second fractions differ by two orders of magnitude). Figure 3 shows that the adsorption properties of the bottom hardly affect the deposition rates of the first two (largest) fractions. However, their effect on the deposition of fine fractions is substantial. In the case of a completely adsorbing bottom (curve *1* in Fig. 3), the deposition rates of the fourth and fifth fractions are nearly completely determined by vertical turbulent diffusion. At the same time, with no diffusive flux at the bottom (curve *2*) in the limit as $\tau \longrightarrow \infty$, the value of W is determined by the hydraulic coarseness of the finest fraction.

In reality, the largest fractions deposit in the near-field region, where the model of [3, 4] based on the advection–diffusion equation is not completely adequate to the phenomenon under consideration. For example, while sinking to the bottom, large-fraction particles can entrain particles of finer fractions (so-called "lump effect") and locally change the dynamic characteristics of the water flow. Nevertheless,

neglecting the stirring up effect produced by large particles falling on the bottom (this effect has to be simulated separately), the model under the conditions of the given scenario yields conservative estimates (upper bounds) for the distribution of the depth-averaged suspension concentration in the far-field region.

4. SIMULATION TECHNIQUE

The computations were based on the stochastic discrete cloud method. Its features and the underlying assumptions can be found in [4]. In the present version of this method, the suspension distribution in the water area is represented by a collection of "elliptic" discrete clouds with the following Gaussian distribution of the depth-averaged suspension concentration:

$$C = \frac{m(t)}{2\pi H(\mathbf{x}_0(t))\sigma'_{1C}(t)\sigma'_{2C}(t)}\exp\left(-\frac{x_1'^2}{2\sigma_{1C}'^2(t)} - \frac{x_2'^2}{2\sigma_{2C}'^2(t)}\right). \quad (4)$$

Here, m is the current mass of the suspension in a cloud and $\mathbf{x}_0$ are the coordinates of the cloud center in the global coordinate system. The primed letters denote the local coordinates measured from the center of the cloud (x'_1 in the direction of the water motion and x'_2 in the perpendicular direction). Each cloud is characterized by the time t_0 of its emergence and by the initial variances $\sigma_{1C0}'^2$ and $\sigma_{2C0}'^2$.

At each time step $\Delta t = t_{n+1} - t_n$, the centers $\mathbf{x}_0$ of the clouds move together with the water and experience normally distributed random walks characterized by the total variance $\sigma_X^2(t)$ (accordingly, the variance of random coordinate increments at each step is equal to $\sigma_X^2(t_{n+1}) - \sigma_X^2(t_n)$). The variances $\sigma_{1C}'^2(t)$, $\sigma_{2C}'^2(t)$, and $\sigma_X^2(t)$ characterizing the computational process are related to the "physical" turbulent variance $\sigma^2(t) = A_3(t - t_0)^3$ determined by the spectrum of horizontal turbulent fluctuations and to the longitudinal variance coefficient K_D by the formulas[3]

$$\frac{d\sigma_{1C}'^2}{dt} = \alpha\frac{d\sigma^2}{dt} + 2K_D, \quad \frac{d\sigma_{2C}'^2}{dt} = \alpha\frac{d\sigma^2}{dt}, \quad \frac{d\sigma_X^2}{dt} = (1-\alpha)\frac{d\sigma^2}{dt}, \quad (5)$$

where $0 \le \alpha \le 1$ is a tuning parameter of the process ($1 - \alpha$ can be interpreted as the degree of stochasticity of the algorithm).

The variation in the cloud mass at each step is calculated by the formula

$$m(t_{n+1}) = m(t_n)\exp\left[-\int_{t_n}^{t_{n+1}}\frac{W(\tau(t))}{H(\mathbf{x}_0(t))}dt\right] = m(t_n)\exp[F(\tau_n) - F(\tau_{n+1})], \quad F(\tau) = \frac{1}{u_*}\int_0^\tau W(\tau')d\tau',$$

where W is the effective hydraulic coarseness and τ is dimensionless time (3).

The total suspension concentration at an arbitrary point at the time t_n is calculated by formula (4) by summation over all the clouds existing at the given time. The increase in the soil deposition thickness due to suspension deposition is computed on a grid introduced in the computational domain. The values

$$\Delta M_{ij}(t_{n+1/2}) = \frac{m(t_n) - m(t_{n+1})}{2\pi\sigma'_{1C}(t_{n+1/2})\sigma'_{2C}(t_{n+1/2})}\exp\left(-\frac{x_{1ij}'^2}{2\sigma_{1C}'^2(t_{n+1/2})} - \frac{x_{2ij}'^2}{2\sigma_{2C}'^2(t_{n+1/2})}\right),$$

are summed in the grid cells (i, j) for all clouds over the entire computation. Here, x'_{1ij} and x'_{2ij} are the locations of the cell centers in local coordinates tired to the center of a cloud. After the computation is ended, the increase h in the soil deposition thickness in a cell is calculated by the formula $h_{ij} = M_{ij}/[(1 - \varepsilon_0)\rho_0 S_{ij}]$, where M_{ij} is the mass of sediments accumulated in the cell and S_{ij} is the area of the cell.

To complete the formulation of the algorithm, we need to determine the initial position of the cloud center $\mathbf{x}_0(t_0)$, its initial mass $m(t_0)$, $\sigma_{1C}'^2(t_0)$, $\sigma_{2C}'^2(t_0)$, and $\sigma_X^2(t_0)$. This is performed as follows. A dumping

[3] Note that, in contrast to [4], where the effect of the longitudinal variance was simulated by a stochastic method, in this paper, the longitudinal variance is described by varying one of the sizes of a discrete elliptic cloud.

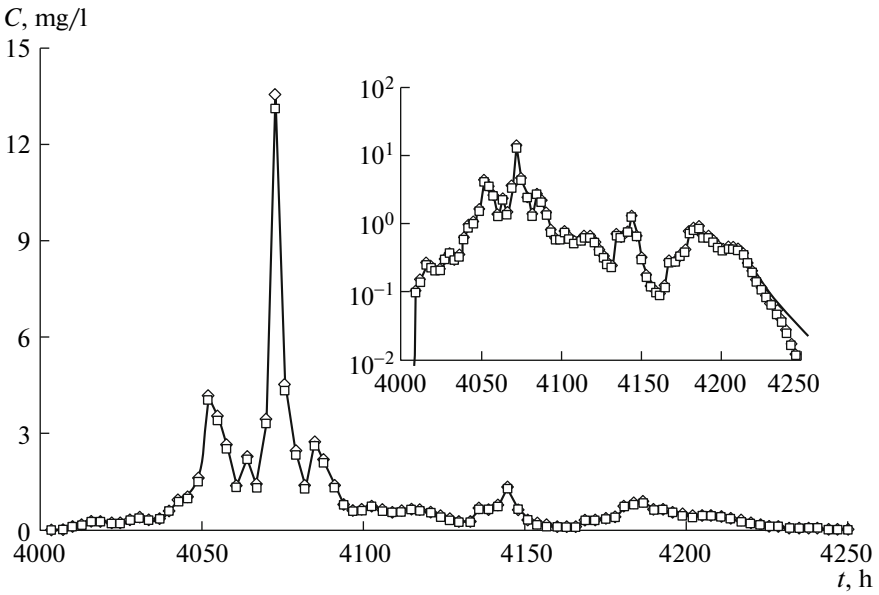

Fig. 4.

event occurring at the time t_0 is simulated by the simultaneous generation of N_p discrete clouds with suspension masses $m_k(t_0) = M_0/N_p$ and with centers $\mathbf{x}_{0k}$ randomly distributed about the dumping point. The values $\mathbf{x}_{0k}$ are generated using the normal distribution with the variances $\sigma_{X1}^2 = (1-\alpha)\sigma_{10}^2$ and $\sigma_{X2}^2 = (1-\alpha)\sigma_{20}^2$ along the corresponding axes, while the initial variances of the substance in each cloud are set equal to $\sigma_{1C}'^2(t_0) = \alpha\sigma_{10}^2$ and $\sigma_{2C}'^2(t_0) = \alpha\sigma_{20}^2$ (see (1)).

For $\alpha = 1$, the algorithm described is the discrete cloud method, in which $N_p = 1$. Each dumping event is simulated by a single discrete cloud, $\mathbf{x}_0(t_0)$ is the dumping point, $m(t_0) = M_0$, $\sigma_{1C}'^2(t_0) = \sigma_{10}^2$, $\sigma_{2C}'^2(t_0) = \sigma_{20}^2$, and $\sigma_X^2(t_0) = 0$.

The limit $\alpha \longrightarrow 0$ corresponds to the discrete particle method (in the absence of longitudinal variance, when $K_D = 0$ in (5)). (If $K_D \neq 0$, this case can be called the discrete interval method.)

Obviously, the discrete cloud method is most efficient in terms of computational costs. However, it requires that the hydrodynamic fields be sufficiently homogeneous; i.e., they must vary little at distances on the order of the cloud size, which increases with time. Since this assumption cannot be verified in practice, a more convenient technique is to estimate the reliability of the results via computations with successively decreasing values of α (see [4]).

Note also that the number of discrete clouds in practical computations may be very large (10^5 and more). Therefore, to minimize the computational costs, it is extremely important to find a criterion according to which a given cloud can be eliminated from the list of processed clouds. In this paper, a cloud is assumed to be completely dissipated if the mean suspension concentration $\bar{C}$ in the cloud at the time t_n satisfies the condition

$$\bar{C}(t_n) = \frac{m(t_n)}{\sigma_{1C}'(t_n)\sigma_{1C}'(t_n)H(\mathbf{x}_0(t_n))} < \frac{C_{\min}}{N_p}, \tag{6}$$

where $C_{\min}$ is a constant chosen so as to ensure satisfactory accuracy of the numerical results, including the regions of low suspension concentrations of order 1 mg/l. Clearly, $C_{\min} \leq 0.1$ mg/l.

5. NUMERICAL RESULTS

First, we describe the results of test computations that were used to determine the admissible values of Δt and $C_{\min}$ in (6). In these computations, several control points were chosen near the dumping area, at

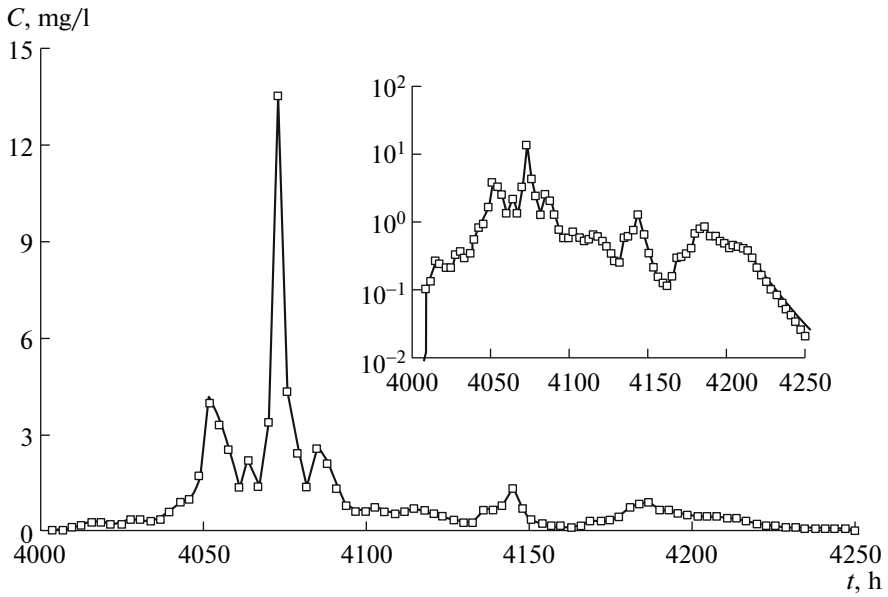

Fig. 5.

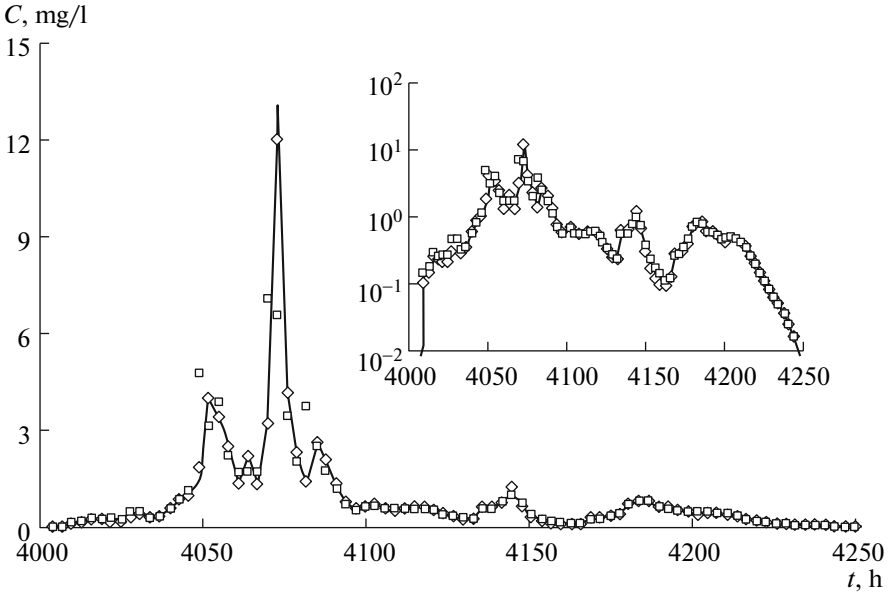

Fig. 6.

which we analyzed the dynamics of the calculated suspension concentration and its dependence on the indicated parameters. Figure 4 presents an example of this dependence at a control point located 500 m away from the southern boundary of the dumping area (see Fig. 1) on linear and logarithmic scales along the vertical axis. The computations were performed with the parameters $\alpha = 1$ and $N_p = 1$ (discrete cloud method) for $C_{\min} = 10^{-2}$ mg/l, $\Delta t = 3.6$ s (circles); $C_{\min} = 10^{-3}$ mg/l, $\Delta t = 3.6$ s (solid curve); and $C_{\min} = 10^{-2}$ mg/l, $\Delta t = 36$ s (squares). An analysis of these test computations suggests that $C_{\min} = 10^{-2}$ mg/l and $\Delta t = 36$ s are sufficient to ensure the acceptable accuracy of the suspension concentration for values of up to 0.1 mg/l.

The second series of computations was used to detect the influence exerted on the result by a spatial inhomogeneity in the current velocity field. For $C_{\min} = 10^{-2}$ mg/l and $\Delta t = 36$ s, Fig. 5 compares the numer-

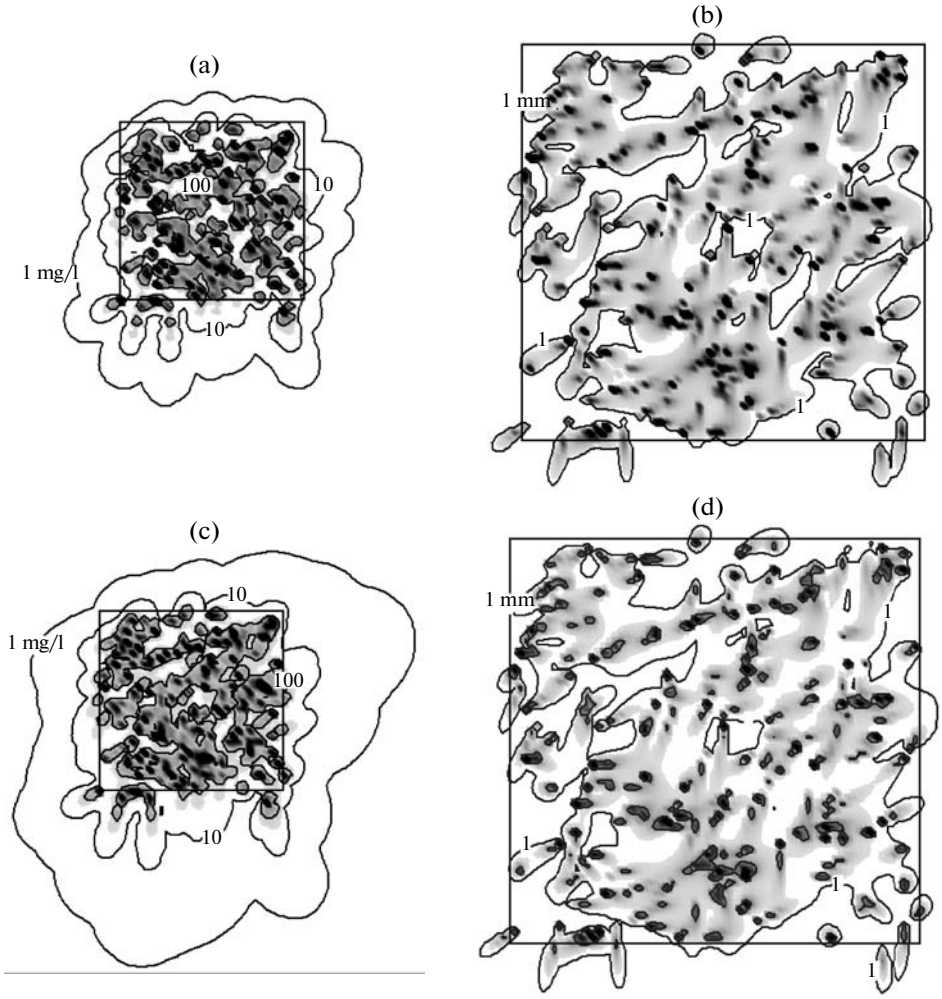

Fig. 7.

ical results produced by the discrete cloud method (heavy line) and the stochastic method with $\alpha = 0.3$ and $N_p = 1000$ (squares). The results coincide nearly completely, which means that, under the considered conditions, the spatial homogeneity of the velocity field is sufficiently high, so the more efficient discrete cloud method can be used without introducing a large error.

Figure 6 shows the numerical results obtained for $\gamma = 0$ (heavy lines), 0.45 (circles), and 10 (squares). It can be seen that the influence of the longitudinal variance becomes noticeable only for unreally large values of γ. The absence of the influence of the longitudinal variance in this case is explained by the low current velocities and the small water depth in the dumping region.

Finally, Fig. 7a depicts the calculated fields of maximal concentrations (i.e., concentrations attained at least once at a given point of the water area in the course of the entire work). Figures 7b and 7d show the increased thickness of the deposited soil. The computations were performed in the case of a completely adsorbing bottom (Figs. 7a, 7b) and with zero diffusive fluxes at the bottom (Figs. 7c, 7d). It can be seen that the adsorption properties of the bottom have a large effect on the area of the spread of the fine suspended substance. At the same time, the thickness of soil deposits up to 1 mm is barely independent of these properties.

CONCLUSIONS

Let us present some data characterizing the speed of the computations.

The computations were performed on a 2.4 GHz Windows XP Pentium 4 computer. The code was written in Delphi 6 Object Pascal.

It was found that the computational costs were insignificant when the suspension concentrations were computed only at several control points. For example, the version with the parameters $\alpha = 1$, $C_{\min} = 10^{-2}$ mg/l, $\Delta t = 36$ s, and $N_p = 1$, which, according to the above test computations, ensure an acceptable accuracy, required CPU time of about $t_{\mathrm{CPU}} = 1$ s. The maximum number of clouds simultaneously participating in a run was only 18. However, the CPU time increased considerably if we needed to compute concentration and sediment fields. For example, on a grid consisting of 100×100 cells, the necessary CPU time was $t_{\mathrm{CPU}} \approx 11$ min. Naturally, as the degree of stochasticity of the algorithm increased (with decreasing α), the necessary CPU time increased as well. For example, for $\alpha = 0.3$, $C_{\min} = 10^{-2}$ mg/l, $\Delta t = 36$ s, and $N_p = 1000$, even without computing the concentration and sediment fields, the CPU time was $t_{\mathrm{CPU}} \approx$ 54 min (while the maximum number of clouds simultaneously participating in a run was about 71000). Nevertheless, these values seem fairly acceptable for practical computations.

Thus, the numerical results presented in this paper demonstrate the good performance and efficiency of the technique developed for the simulation of suspended substance transport on the ocean shelf.

ACKNOWLEDGMENTS

This work was supported by the Russian Foundation for Basic Research (project nos. 08-07-00118 and 08-01-00435) and by the Department of Mathematical Sciences of the Russian Academy of Sciences (basic-research program no. 3).

REFERENCES

1. L. F. Richardson, "Atmospheric Diffusion Shown on a Distance-Neighbor Graph," Proc. R. Soc. Ser. A **110**, 709–720 (1926).
2. A. Okubo and R. V. Ozmidov, "Empirical Dependence of the Horizontal Diffusion Coefficient on the Phenomenon Scale," Fiz. Atm. Okeana **6**, 534–536 (1970).
3. V. N. Koterov and Yu. S. Yurezanskaya, "Simulation of Suspended Substance Dispersion on the Ocean Shelf: Effective Hydraulic Coarseness of Polydisperse Suspension," Zh. Vychisl. Mat. Mat. Fiz. **49**, 1306–1318 (2009) [Comput. Math. Math. Phys. **49**, 1245–1256 (2009)].
4. V. N. Koterov and Yu. S. Yurezanskaya, "Simulation of Suspended Substance Transport on the Continental Shelf: Horizontal Dispersion," Zh. Vychisl. Mat. Mat. Fiz. **50**, 375–387 (2010) [Comput. Math. Math. Phys. **50**, 357–368 (2010)].
5. A. Gill, *Atmosphere–Ocean Dynamics* (Academic, New York, 1982; Mir, Moscow, 1986), Vol. 2.
6. E. Kalnay, M. Kanamitsu, R. Kistler, et al., "The NCEP/NCAR 40-Year Reanalysis Project," Bull. Am. Meteor. Soc. **77**, 437–470 (1996).
7. J. Nihoul, *Modeling of Marine Systems* (Gidrometeoizdat, Leningrad, 1978) [in Russian].